วารสารวิชาการเทคโนโลยีอุตสาหกรรม (The Journal of Industrial Technology)
ISSN (online): 2697-5548
DOI: 10.14416/j.ind.tech.2026.04.012

บทความวิจัย

Natural Heat Convection Analysis on Boundary layer and Apply Utilization to Inclined Solar Collector

Sriwichai Susuk[1*], Rachain Visutthipat[1], Weerayuth Promjan[2] and Natsacha Inchoorrun[2]

[1] Biodiversity Research Center, Research and Development Group for Bio-Industries, Thailand Institute of Scientific and Technological Research (TISTR) 12120

[2] Expert Center of Innovative Health Food, [Inno-Food], Research and Development Group for Bio-Industries, Thailand Institute of Scientific and Technological Research (TISTR) 12120

[*] Corresponding author, E-mail: sriwichai@tistr.or.th

Received: 7 August 2025; Revised: 4 February 2026; Accepted: 9 March 2026
Online Published: 21 April 2026

Abstract: Natural convection heat transfer driven by solar energy is a sustainable and environmentally friendly method for drying agricultural products, representing a critical mechanism in various solar dryer applications (free energy). This study experimentally investigates the laminar natural convection heat flow along an inclined solar collector under conditions approximating steady-state operation during peak sunlight hours. The research evaluates the velocity and temperature distributions on an inclined glass plate based on the development of thermal boundary layers. In addition to the limiting cases of flow adjacent to surfaces. Results indicate that the natural convection heat transfer coefficient ranges from 5.2 to 6.6 $W/m^2°C$, while the collected heat energy ranges from 150 to 610 J/s, achieving a collector efficiency between 23.9% and 38.3%. The dry air flow rate was observed to be between 0.016 and 0.024 m^3/s during daylight hours (local time). Under a fixed solar collector tilt angle of 25° and solar irradiation ranging from 217.8 W/m^2 to 552.7 W/m^2, the average Nusselt and Rayleigh numbers were determined to be 221.7 and $6.7x10^9$, respectively. Finally, load tests demonstrated a drying rate ranging from 0.07 to 1.45 kg/hr, which varied significantly based on local climatic conditions and the time of day.

Keywords: Natural convection heat transfer; Sustainable renewable energy; Laminar natural convection heat; Heat transfer coefficient; Nusselt number; Rayleigh number

วารสารวิชาการเทคโนโลยีอุตสาหกรรม (The Journal of Industrial Technology)
ISSN (online): 2697-5548
DOI: 10.14416/j.ind.tech.2026.04.012

1. Introduction

Solar radiation is a sustainable energy source that is both abundant and environmentally friendly. Solar drying is a superior alternative to traditional open-air drying, as it protects products from contaminants like dust and insects while maintaining higher nutrient levels and accelerating the dehydration process. Drying involves the reduction of moisture through vaporization, a process often driven by buoyancy-induced fluid flow known as natural convection. In solar collectors, heat transfer occurs between the solid absorber surface and the surrounding air, resulting in the development of a thermal boundary layer. Natural convection heat transfer is driven by non-uniform density distributions within a fluid caused by temperature gradients [1-3]. For an inclined plate, the laminar flow region can be analyzed by modifying the gravitational terms in dimensionless governing equations. Key dimensionless quantities used to correlate heat transfer coefficients include the Nusselt number (Nu), Rayleigh number (Ra), Grashof number (Gr), Reynolds number (Re), and Prandtl number (Pr). Specifically, the Pohlhausen equation is utilized to solve for air velocity within the boundary layer of laminar flow on inclined surfaces. Literature Review, previous studies have analyzed these dynamics extensively. Dehghani et al. [4], Alzwayi and Paul [7] demonstrated that temperature variations significantly affect air transition on isothermal plates, particularly below 60°C. Hollands et al. [8] found that for tilt angles up to 70°, heat transfer rates can be predicted by replacing Ra with Ra.($\cos\omega$). Furthermore, researchers like González-Bárcena et. al., [9] Mehrtash and Tari [10] have utilized computational fluid dynamics (CFD) to refine air flow rate and temperature field models for inclined sinks. Mustafa and Neama [11] observed that absorber plate temperatures are directly proportional to solar radiation, noting a peak temperature of 82°C at a 30° tilt angle. Despite these findings, there remains a need for a comprehensive evaluation of natural convection correlations specifically tailored for inclined glass solar collectors under specific tropical climatic conditions like those in Thailand.

Objectives and Significance, this research performs a systematic evaluation of natural convection correlations and heat transfer coefficients. This study assumes steady, incompressible laminar flow to simplify the boundary layer analysis for the intended application. While natural convection can be unsteady, the steady-state assumption is applied here to predict the mean performance of the collector under constant solar irradiance. The primary objective is to examine dimensionless correlations (Nu, Ra, Gr, Re, Pr) and the Pohlhausen equation to optimize heat and mass flow rates. Unlike previous studies that examine various angles, this work focuses on the

วารสารวิชาการเทคโนโลยีอุตสาหกรรม (The Journal of Industrial Technology)
ISSN (online): 2697-5548
DOI: 10.14416/j.ind.tech.2026.04.012

performance at a fixed tilt angle of 25° (with the peak thermal output, comparative of 20° and 30°) to determine the effectiveness of the collector for agricultural drying at standard pressure.

2. Experimental detail; material and method

2.1 Description of solar collector inclined plate

Figure 1 illustrates the schematic cross-sectional view of the inclined solar collector and the development of the boundary layer. The geometric model features a glass plate with dimensions of 2.4 m in length, 1.2 m in width, and 6 mm in thickness. Supported by a mild steel frame, the structure is designed to maximize solar gain during daylight hours to evaluate the buoyancy-driven boundary layer and air mass flow rate under natural convection at constant pressure. The collector was oriented at a fixed tilt angle of 25° from the horizontal. This specific angle was selected based on a preliminary empirical study comparing tilt angles of 20°, 25° and 30° at the experimental site. The results demonstrated that the 25° inclination yielded the highest surface plate temperature (T_p) and maximum heat energy absorption for Pathum Thani, Thailand. This increased surface temperature is directly proportional to the heat energy absorbed, which effectively drives the natural buoyancy mechanism required for analyzing the laminar boundary layer.

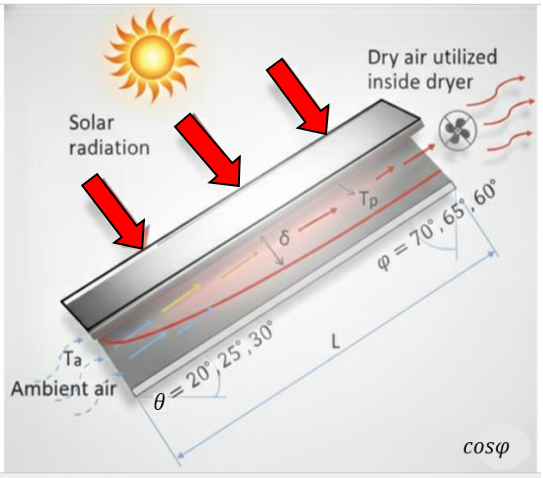

Fig. 1 Schematic of inclined solar collector

2.2 Experimental Setup and Instrumentation

The measurement were carried out at Pathum Thani, Thalland a latitude of 14°0'48.46" North and longitude of 100°31'49.76" East. from January 2022 to December 2024. Testing was carried out under no-load conditions between 8 a.m. and 4 p.m. daily. Air temperatures were measured along the interior surface of the glass plate using five designated points positioned along a central axis (red line), each spaced approximately 20 cm apart, as shown in the schematic diagram in Figure 2. The thermal profile was established by recording parameters hourly using a solar power meter (SM206-SOLAR, uncertainty ±5%) for Solar Radiation and an Infrared thermometer (TM 1803, accuracy ±2%) for Ambient (T_a) and Surface (T_p) Temperatures. Air velocity was monitored using an anemometer (CBzSGHJ001)

วารสารวิชาการเทคโนโลยีอุตสาหกรรม (The Journal of Industrial Technology)
ISSN (online): 2697-5548
DOI: 10.14416/j.ind.tech.2026.04.012

with an accuracy of ±3%, ensuring precise data on convective cooling effects. Humidity levels were tracked via a temperature & humidity meter (L563A) with a ±5% RH margin, while Moisture Content was determined using an OHAUS MB23 Moisture meter (repeatability ±0.05%), all detail according to Table 2. These high-precision instruments ensure the reliability of the collected data across varying environmental conditions throughout the study period. All measurements were conducted in accordance with the manufacturer's calibration standards to minimize potential systematic errors in the thermal analysis.

3. Equations and mathematics analysis

3.1 Analysis mechanism heat solar energy

To comprehensively understand the natural buoyancy mechanism of a heated plate, a coupling between energy and mass transfer must be established (according to Figure 3). These coefficients are parameterized as functions of dimensionless quantities. Similar to the ideal gas law, the density of dry air is a critical factor in the absorption of surrounding moisture [5, 12-15].

3.2 Thermophysical Properties and Reference Temperature

The thermo-physical properties of gas are significantly influenced by variations in temperature and pressure. In this study, natural convection heat transfer occurs between the collector surfaces

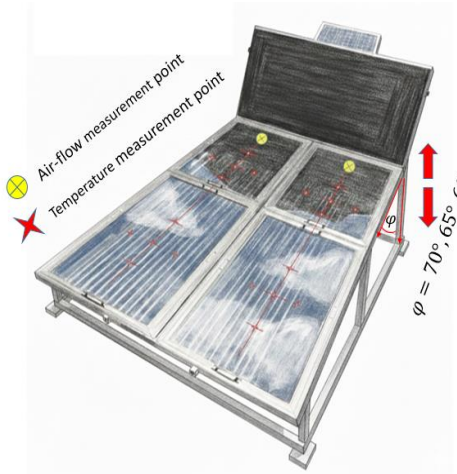

Fig. 2 Experimental setup solar collector plate

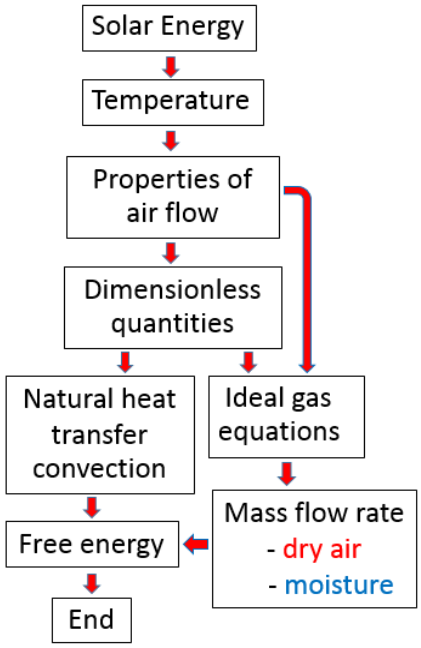

Fig. 3 Schematic chart of analysis

and the ambient air. This process induces a flow of dry air, driven by density gradients within the boundary layer. To simplify the numerical

วารสารวิชาการเทคโนโลยีอุตสาหกรรม (The Journal of Industrial Technology)
ISSN (online): 2697-5548
DOI: 10.14416/j.ind.tech.2026.04.012

analysis, the air is assumed to be a steady, laminar, and incompressible fluid [9]. The relevant physical properties are calculated using equations (1-6) evaluated at the reference temperature.

$$\Pr(T) = 0.804 - 3.25\times10^{-4}T_f \quad (1)$$

$$\mu(T) = \frac{1.458\times10^{-6}\times T_f^{3/2}}{T_f + 110.4} \quad (2)$$

$$k(T) = \frac{2.68151\times10^{-3}T_f^{3/2}}{T_f + 245.4\times10^{-12/T_f}} \quad (3)$$

$$C_p = \frac{\Pr.k}{\mu} \quad (4)$$

$$\rho_a = \frac{P_A}{R_A\times T_f}\text{; Considering the air as an ideal gas} \quad (5)$$

$$T_f = \frac{T_p + T_a}{2} \quad (6)$$

The boundary-layer thickness for laminar free convection and the mean flow velocity can be determined using Equations (7) and (8), respectively [7].

$$\frac{\delta}{L} = 3.93\Pr^{-1/2}(0.92+\Pr)^{1/4}\left(\frac{Ra}{\Pr}\right)^{-1/4} \quad (7)$$

$$\nu = \frac{\mu.Gr^{1/2}}{\rho.L} \quad (8)$$

3.3 Governing Equations for Dimensionless Quantities

The heat transfer characteristics and flow behavior are evaluated using dimensionless parameters. According to established correlations [5,13,14], these quantities are defined as follows:

Nusselt Number (Nu), Represents the ratio of convective to conductive heat transfer across a fluid boundary layer. Specifically, it characterizes the enhancement of heat transfer due to fluid motion compared to the heat transfer that would occur through pure conduction in a stationary fluid layer of the same thickness.

$$\bar{N}_u^{1/2} = \left[0.825 + \frac{0.387Ra^{1/16}}{\left[1+(0.492/\Pr)^{9/16}\right]^{8/27}}\right] \quad (9)$$

Rayleigh Number (Ra), Characterizes the flow regime and the strength of buoyancy-driven flow in free convection.

$$R_a\cos\varphi = \Pr\times G_r\cos\varphi \quad (10)$$

Grashof Number (Gr), Relates the buoyancy force to the viscous force acting on the fluid

$$G_r = \frac{L^3 g\beta\rho^2(T_p - T_a)}{\mu^2} \quad (11)$$

$$\beta = \frac{1}{(T_f + 273.15)} \quad (12)$$

วารสารวิชาการเทคโนโลยีอุตสาหกรรม (The Journal of Industrial Technology)
ISSN (online): 2697-5548
DOI: 10.14416/j.ind.tech.2026.04.012

Reynolds Number (Re), Defined for internal or forced flow components within the system.

$$\mathrm{Re} = \left(\frac{\bar{N}_u}{0.664\,\mathrm{Pr}^{1/3}}\right)^2 \quad (13)$$

Convective heat transfer coefficient (hc), derived from the Nusselt number.

$$h_c = \frac{k\bar{N}_u}{L} \quad (14)$$

3.4 Solar Collector Design and Energy Analysis

The intensity of solar radiation, natural convection characteristics, and required thermal energy are evaluated using Equations (15-18). Previous research by Ayad et al. suggested that a tilt angle of 30° maximizes thermal energy gain. However, empirical results from the present study conducted at a latitude of 14°0'48.46" N demonstrate that a tilt angle of 25° yields superior thermal performance. This experimental finding aligns with the theoretical calculations derived from Equation (16). Furthermore, the correlation was validated by modifying the Rayleigh number (Ra) in Equation (10) to account for the inclination, substituting it with Ra.cos(65°). This adjustment accounts for the reduction in the buoyancy force component

$$\theta = 10^{\circ} + Lat\phi \quad (15)$$

$$E_i = I \times A \quad (16)$$

$$\eta_C = \frac{\dot{q}_c}{E_i} \times 100 \quad (17)$$

$$\dot{q}_c = h_c \times A \times (\Delta T) \quad (18)$$

3.5 Pressure Analysis

The total vapor pressure of water at the operating temperature, along with the air properties derived from the ideal gas law, can be evaluated using Equations (19-23) [15,16]. These equations are essential for determining the humidity ratio and the thermodynamic behavior of the moist air within the drying system.

$$P_s(T) = \exp\left[25.317 - \frac{5144}{T_f + 273.15}\right] \quad (19)$$

$$P_A V_A = m_a R_A (T_f + 273.15) \quad (20)$$

$$P_s V_w = m_w R_w (T_v + 273.15) \quad (21)$$

$$\frac{m_w}{m_a} = 0.622 P_s / (P_{atm} - P_s) \quad (22)$$

$$\frac{m_w}{m_a} = \frac{\frac{P_s V}{R_w (T_f + 273.15)}}{\frac{P_A V}{R_A (T_f + 273.15)}} \quad (23)$$

วารสารวิชาการเทคโนโลยีอุตสาหกรรม (The Journal of Industrial Technology)
ISSN (online): 2697-5548
DOI: 10.14416/j.ind.tech.2026.04.012

4. Results and Discussions

4.1 Solar Radiation and Thermal Performance

Table 1 and Figure 4 present the comprehensive hourly performance of the solar collector under varying tilt angles 20˚, 25˚, 30˚. The incident solar irradiance intensified from 218 W/m^2 in the early morning to a peak of 553 W/m^2 at 1 p.m., this peak irradiance directly influenced the absorber's thermal gain, with the 25° tilt angle consistently yielding the highest glass plate temperatures (T_p) throughout the day. Specifically, at the solar noon peak, the 25° configuration achieved a maximum T_p of 72.4°C, surpassing the 20° (71.8°C) and 30° (71.3°C) orientations. This variance confirms that a 25° inclination optimizes the angle of incidence, thereby maximizing the capture of beam radiation and minimizing reflective losses during the highest flux periods. Psychrometric analysis and drying Potential, the internal microclimate of the collector showed a superior drying potential compared to ambient conditions. As the solar intensity peaked, the internal relative humidity (RH) plummeted from an initial 32.3% to a minimum of 21.3%, whereas the ambient RH remained significantly higher at 36.7%. Engineering Insight, the observed inverse relationship between T_p and internal RH validates the system's capability to drastically lower the air's partial vapor pressure. This increases the humidity ratio differential between the drying air and the product surface, which is the primary driving force for accelerated mass transfer in solar drying applications.

Table 1 Variation of solar radiation, average film temperature and relative humidity

Time	8 a.m.	9 a.m.	10 a.m.	11 a.m.	12 a.m.	1 p.m.	2 p.m.	3 p.m.	4 p.m.
Solar radiation (W/m^2)	218	298	361	430	486	553	487	406	292
Ambien temperature; T_a,(°C)	31.4	34.4	37.0	39.6	40.9	42.6	41.4	39.3	35.6
Avg. glass plate temperature; T_p,(°C) at 20°	37.2	45.9	52.5	59.7	65.1	71.8	66.0	57.2	47.5
Avg. glass plate temperature; T_p,(°C) at 25°	37.8	46.7	53.8	60.2	65.3	72.4	66.3	57.5	47.6
Avg. glass plate temperature; T_p,(°C) at 30°	36.8	45.5	52.3	59.5	64.8	71.3	65.7	56.8	47.2
%R.H. ambient air	52.8	46.5	43.3	39.2	38.9	36.7	38.4	40.6	43.5
%R.H. inside solar collector	32.3	28.4	26.7	23.8	23.4	21.3	22.4	23.5	25.7

วารสารวิชาการเทคโนโลยีอุตสาหกรรม (The Journal of Industrial Technology)
ISSN (online): 2697-5548
DOI: 10.14416/j.ind.tech.2026.04.012

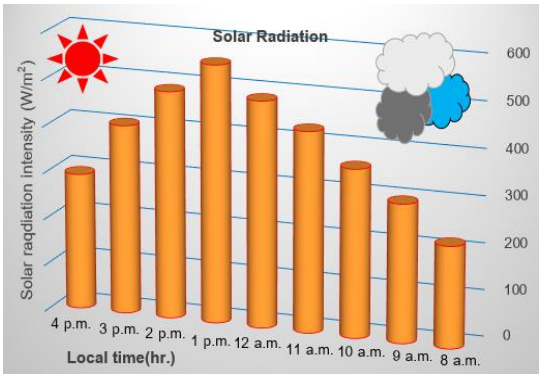

Fig. 4 Variation of mean solar radiation

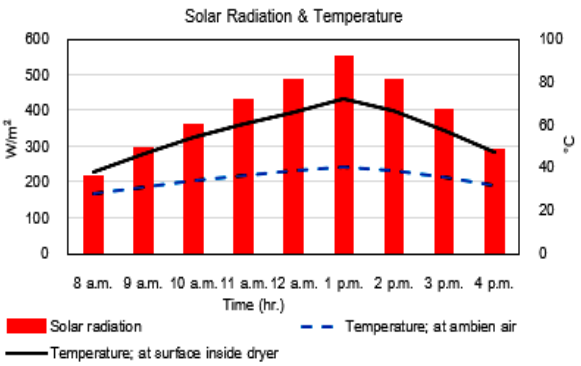

Fig. 5 Variation of solar radiation and Temp.

4.2 Dimensionless Parameters and Flow Characteristics

The correlation between mean temperature and solar radiation is illustrated in Figure 5, both parameters reached their peak at 1 p.m. aligning with the solar noon period where solar irradiance intensity is at its maximum. Throughout the observation period (8 a.m. to 4 p.m.), the temperature of the absorber plate (T_p) consistently exceeded the ambient air temperature (T_a), establishing a sustained thermal gradient (ΔT) that serves as the primary driver for the system's efficiency.

Fluid dynamics and buoyancy, the significant temperature differential creates a localized air density gradient within the collector. According to the principles of fluid mechanics, the reduction in air density near the absorber surface induces a buoyancy force, governed by the Grashof number, which overcomes internal viscous drag.

Passive flow generation, this buoyancy effect establishes a steady-state flow field, where heated air rises via natural convection. This mechanism ensures a continuous mass flow rate of heated air into the drying chamber without the requirement for external mechanical work or parasitic energy consumption.

Energy balance and heat transfer, the synchronized rise of solar radiation and surface temperature validates the high spectral absorptivity of the collector material and the effective minimization of convective and radiative heat losses.

Natural draft optimization, the establishment of a robust natural draft through these density gradients demonstrates that the system is optimized for passive solar thermal gain, utilizing the stack effect to maintain the required velocity for effective moisture removal in drying processes.

วารสารวิชาการเทคโนโลยีอุตสาหกรรม (The Journal of Industrial Technology)
ISSN (online): 2697-5548
DOI: 10.14416/j.ind.tech.2026.04.012

The relationship between the Rayleigh number (Ra) and the Nusselt number (Nu) is illustrated in Figure 6. As dimensionless quantities, they characterize the free convection flow resulting from air density gradients within the collector. This analysis characterizes the transition and effectiveness of convective heat transfer within the solar collector system.

Rayleigh number (Ra) and Buoyancy forces, the Rayleigh number, represented by the red bars, quantifies the ratio of buoyancy-driven forces to viscous and thermal diffusive forces. As the temperature increases from 33°C to a peak of 56°C, Ra increases significantly, reaching values in the range of 8 x 10^9. This high magnitude confirms that the flow within the collector is dominated by natural convection and has likely entered the turbulent regime, which is essential for maximizing air mixing and heat uptake.

Nusselt number (Nu) and Convective efficiency, the Nusselt number, indicated by the black line, represents the ratio of convective to conductive heat transfer across the boundary layer. The graph shows Nu rising in tandem with temperature and Ra, peaking at approximately 230. This peak validates that the convective heat transfer is most efficient when the absorber plate reaches its maximum operating temperature, directly correlating with the period of peak solar irradiance identified previously.

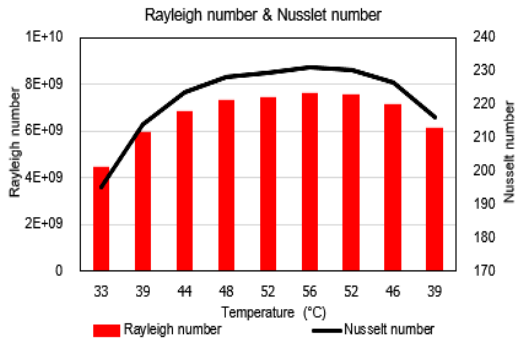

Fig. 6 Variation of Rayleigh and Nusselt number

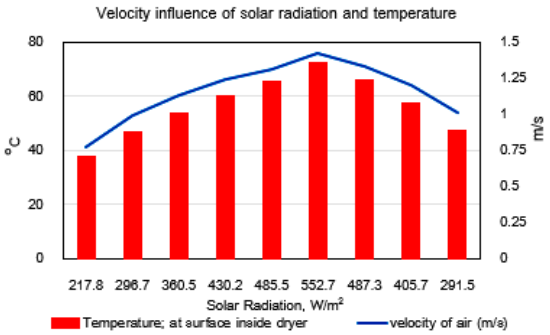

Fig. 7 Variation of velocity

Figure 7 illustrates the velocity influence of solar radiation and temperature shows a direct correlation between solar irradiance and air velocity as solar radiation peaks at 552.7 W/m², the absorber plate temperature reaches its maximum. This creates a significant temperature difference between the air inside the collector and the ambient air. This temperature rise decreases the air density, creating a pressure head that drives the natural draft. The resulting velocity (peaking at 1.4 m/s) is the physical manifestation

วารสารวิชาการเทคโนโลยีอุตสาหกรรม (The Journal of Industrial Technology)
ISSN (online): 2697-5548
DOI: 10.14416/j.ind.tech.2026.04.012

of the system's ability to maintain a continuous flow for moisture displacement without mechanical assistance.

Figure 8 illustrates the mean convective heat transfer coefficient (h_c) and the resulting convective heat transfer rate. The heat transfer coefficient fluctuated between 5.2 and 6.5 W/m²°C, while the convective heat rate ranged from 150 to 610 J/s. This heat exchange occurs at the glass surface, driven by the buoyancy-induced motion of air (natural convection). These processes are significantly influenced by the film temperature (T_f), which ranged between 33°C and 56°C.The results indicate that the convective rate peaks at the maximum film temperature, reflecting the increased buoyancy forces. The most significant thermal activity was observed at 1 p.m., where the performance is governed by the peak incident heat flux. During this period, the intensified temperature gradient enhances the convective flow, leading to the maximum observed heat transfer rates.

Figure 9 illustrates the relationship between the component volumetric flow rates and the film temperature (T_f) within the solar thermal system. The observed airflow is a direct consequence of buoyancy-driven flow fields induced by temperature-dependent density gradients, a process fundamental to natural convection. As the solar-heated film temperature increased from 33°C to 56°C, the resulting convective heat rate

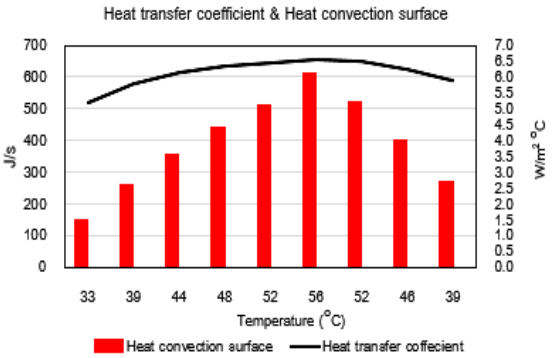

Fig. 8 Variation of heat transfer coefficient and heat convection surface

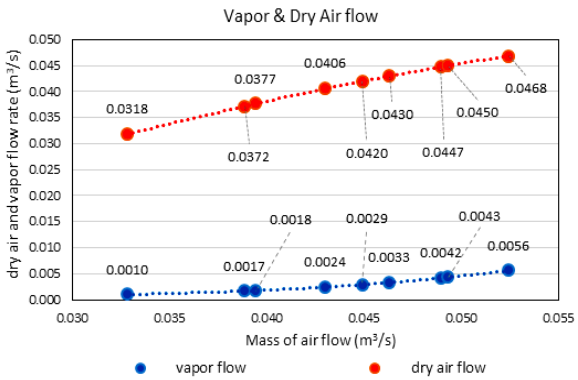

Fig. 9 Variation of volumetric flow rate characterization of moist air components

rose significantly from 150 to 610 J/s. Concurrently, the total volumetric flow rate representing the system's ventilation or drying capacity ranged from 0.033 to 0.052 m^3/s. This total flow is comprised of both dry air and water vapor components, where the mass transfer is strictly governed by the buoyancy regime established by the solar thermal gradient.

วารสารวิชาการเทคโนโลยีอุตสาหกรรม (The Journal of Industrial Technology)
ISSN (online): 2697-5548
DOI: 10.14416/j.ind.tech.2026.04.012

4.2 Performance Evaluation with Product Load

Figure 10 illustrates the transient response of the solar collector under actual loading conditions from 8 a.m. to 4 p.m., the analysis focuses on the correlation between solar irradiance, theoretical mass flow rates derived from the equations, and the measured drying rate.

The solar radiation (red line) peaked at approximately 550 W/m^2 around 1 p.m. This peak directly correlates with the maximum mass flow rate, validating that the natural convection mechanism is highly sensitive to the thermal gradient established by the solar flux. The analytical mass flow rate (black line) and the actual drying test with load (blue line) exhibit a high degree of synchronization. The theoretical model, utilizing dimensionless groups (Gr and Ra), effectively predicts the trend of the air movement, though the experimental drying rate is lower due to the latent heat of vaporization and the internal resistance of the product load. The data confirms that the fixed tilt angle of 25° successfully concentrated solar energy to achieve a peak mass flow rate of approximately 2.2 kg/hr (analytical) and 1.5 kg/hr (experimental) during solar noon. This reinforces the maximizing buoyancy.

Figure 11 Illustrates experimental results demonstrate a high level of synergy between the collector's thermal performance and the drying of the banana 10 kg initial load (flattening them to a uniform thickness of approximately 1 cm). By

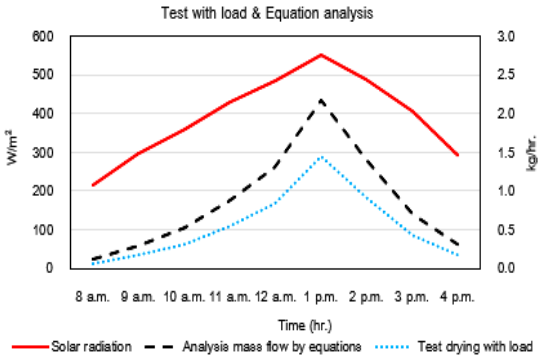

Fig. 10 Variation of solar radiation, analytical mass flow, and experimental drying rate

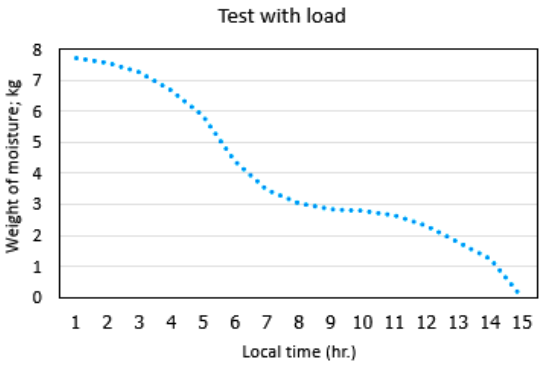

Fig. 11 Variation of moisture loss under natural convection solar drying

utilizing an optimized 25° tilt angle, the system effectively managed the transition of the product from an initial 80% to a final 12% moisture content (w.b.) over a cumulative around 15-hour period.

First day: The acceleration phase (hours 1–8). The system experienced the peak solar radiation of 550 W/m². As the experimental mass flow reached 1.5 kg/hr at 1 p.m., this high airflow effectively stripped the free moisture from the

วารสารวิชาการเทคโนโลยีอุตสาหกรรม (The Journal of Industrial Technology)
ISSN (online): 2697-5548
DOI: 10.14416/j.ind.tech.2026.04.012

banana surfaces, this is reflected by the sharp drop, where the drying rate was at its maximum due to optimal buoyancy and thermal gain.

Second day: The diffusion phase (hours 9–15). As the process entered the second day, the moisture removal rate slowed down. This is the falling rate period. At this stage, the remaining moisture is bound moisture trapped deep within the banana tissues. Even with a high mass flow, the drying is now limited by internal diffusion rather than external convection.

Table 2 Detailed specifications of experimental instrumentation

Measurement Parameter	Measurement Range	Accuracy
Solar Radiation	0.1–399.9 W/m^2	± 5%
Ambient (T_a) & Surface (T_p)	-50°C-500°C	± 2%
Air Velocity	0.3–30.0 m/s	± 3%
Relative Humidity	10%–95% RH	± 5% RH
Moisture Content	0.00%–100%	± 0.05%

5. Conclusions

This study demonstrates that a 25° tilt angle is the critical design parameter for maximizing solar absorption and natural convection. The system achieved a high efficiency thermal regime, characterized by a Rayleigh number (Ra) approximately 8 x 10^9 and a peak Nusselt number (Nu) of 230. These values confirm that buoyancy forces effectively overcame viscous resistance, maintaining a consistent mass flow rate of 0.024 m³/s without external assistance. Thermodynamic analysis showed a peak thermal efficiency of 38.3% and a maximum heat transfer coefficient (h_c) of 6.6 W/m²°C, converting incident radiation (up to 610 J/s) into useful thermal energy while minimizing heat losses. In practical load tests with 10 kg of agricultural product, the collector successfully reduced moisture content from 80% to 12%. This process followed a distinct two-stage drying characteristic, an initial acceleration phase (air velocity up to 1.4 m/s) followed by a stable diffusion phase.

Ultimately, the results validate this inclined solar collector as a high-performance, zero-emission solution, offering a technologically viable and sustainable pathway for renewable energy based agriculture. Beyond thermal performance, this system represents a significant in energy conservation. By utilizing passive natural convection, the collector eliminates the need for electricity. This translates into a sustainable and technologically viable pathway for low-carbon agriculture, aligning with global energy conservation mandates and the transition toward a circular bio-economy.

วารสารวิชาการเทคโนโลยีอุตสาหกรรม (The Journal of Industrial Technology)
ISSN (online): 2697-5548
DOI: 10.14416/j.ind.tech.2026.04.012

6. Nomenclature

Nu	dimensionless	Nusselt number
Ra	dimensionless	Rayleigh number
Pr	dimensionless	Prandtl number
Gr	dimensionless	Grashof number
Re	dimensionless	Reynolds Number
g	m/s^2	Acceleration due to gravity
ϕ	°N	Latitude of collector location
β	1/°K	Coefficient of thermal expansion
ρ	kg/m^3	Density
ΔT	°C	Temperature difference; (Tp-Ta)
T_a	°C	Temperature ambient air
T_p	°C	Surface plate's temperature
T_v	°C	Vapor temperature
T_f	°C	Film temperature
v	m/s	Velocity of air
δ	m	Boundary-layer thickness
A	m^2	Total collector area
η_c	%	Efficiency Thermal collector
m_w	g	Mass of vapor removed (moisture)
V	m^3	Volume of air
m_a	g	Mass of air
P_{atm}	Pa	Pressure of ambient,1 atm
P_A	Pa	Pressure of air
P_s	Pa	Pressure of steam (moisture)
R_A	J/kg°K	Gas constant = 287.1
R_w	J/kg°K	Moisture constant = 461.5
h_c	$W/m^{2}°C$	Convective heat transfer coefficient
$\dot{q}$	J/s	Heat transfer rate
C_p	kJ/kg˚C	Specific heat of dry air
k	W/m˚C	Thermal conductivity
Ei	W	Solar energy
μ	kg/m.s	Dynamic viscosity
L	m	Length

7. Acknowledgements

The authors would like to express their sincere gratitude to the Biodiversity Research Center and the Research and Development Group for Bio-Industries at the Thailand Institute of Scientific and Technological Research (TISTR) for providing the research facilities, equipment, and technical support that made this work possible.

วารสารวิชาการเทคโนโลยีอุตสาหกรรม (The Journal of Industrial Technology)
ISSN (online): 2697-5548
DOI: 10.14416/j.ind.tech.2026.04.012

8. References

[1] T.A. Yassen, M.S.M. Al-Jethelah and H.S. Dheyab, Experiment study of innovative indirect solar dryer, International Journal of Heat and Technology, 2021, 39(4), 1313–1320.

[2] M.C. Ndukwu, E.O. Diemuodeke, F.I. Abam, U.C. Abada, N. Eke-emezie and M. Simo-Tagne, Development and modelling of heat and mass transfer analysis of a low-cost solar dryer integrated with biomass heater: Application for West African Region, 2020, Scientific African, 10, e00615.

[3] G. Habtay, J. Buzas and I. Farkas, Heat transfer analysis in the chimney of the indirect solar dryer under natural convection mode, FME Transactions, 2020, 48, 701–706.

[4] P. Dehghani, D.H. Chaudhari and M.J. DiDomizio, Natural convection on a vertical surface: Direct numerical simulation versus empirical correlations, Journal of Physics: Conference Series, 2024, 2885, 012056.

[5] A. Jaffer, Natural convection heat transfer from an isothermal plate, Thermo, 2023, 3, 148–175.

[6] T. Fujii, H. Imura, Natural convection heat transfer from a plate with arbitrary inclination, Heat and Mass Transfer, 1972, 15(4), 755–767.

[7] A.S. Alzwayi and M.C. Paul, An analytical Investigation of the Physical Dimensions of Natural Convection Flow on a Vertical Heated Plate, Proceedings of the World Congress on Engineering, 2010, 1404–1408.

[8] K.G.T. Hollands, T.E. Unny, G.D. Raithby and L. Konicek, Free convective heat transfer across inclined air layers, Journal of Heat Transfer, 1976, 98(2), 189–193.

[9] D. González-Bárcena, N. Martínez-Figueira, A. Fernández-Soler, I. Torralbo, M. Bayón, J. Piqueras, I. Pérez-Grande, Experimental correlation of natural convection in low Rayleigh atmospheres for vertical plates and comparison between CFD and lumped parameter analysis, International Journal of Heat and Mass Transfer, 2024, 222, 125140.

[10] M. Mehrtash, I. Tari, A correlation for natural convection heat transfer from inclined plate-finned heat sinks, Applied Thermal Engineering, 2013, 51(1-2), 1067–1075.

[11] A.T. Mustafa and M.A. Neama, Natural convection heat transfer on an inclined unglazed solar absorber-plate: Experimental investigation, Conference: AIP Conference Proceedings, 2023, 2530, 090002.

วารสารวิชาการเทคโนโลยีอุตสาหกรรม (The Journal of Industrial Technology)
ISSN (online): 2697-5548
DOI: 10.14416/j.ind.tech.2026.04.012

[12] J.B. Hussein, M.A. Hassan, S.A. Kareem and K.B. Filli, , Design, construction and testing of a hybrid photovoltaic (PV) solar dryer, International Journal of Engineering Research and Science, 2017, 3(5), 1-14.

[13] S.W. Churchill and H.H.S. Chu, Correlating equations for laminar and turbulent free convection from a vertical plate, International Journal of Heat and Mass Transfer, 1975, 18(11), 1323–1329.

[14] Mehmet Daş, E. Alıç and E.K. Akpinar, Numerical and experimental analysis of heat and mass transfer in the drying process of solar drying system, Engineering Science and Technology, an International Journal, 2021, 24, 236–246.

[15] K.N. Çerç, D.B. Saydam and E. Hürdoğan, Estimation of experimental drying performance parameters using polynomial SVM and ANN models, european mechanical science, 2020, 4(3), 123–130.

[16] I.J.G. Berry, Psychometry: Use of standard charts for non-standard air pressure, Building Services Engineering Research and Technology, 1990, 11(2), 73–75.